AENSI Journals

Australian Journal of Basic and Applied Sciences

Journal home page: www.ajbasweb.com

Analysis of Gray Levels for Retinal Image Classification

[1]S. Karthikeyan, [2]Dr. N. Rengarajan

[1]*Associate Professor, Department of ECE, K.S.R. College of Engineering, Tiruchengode, India.*
[2]*Principal, K.S.R. College of Engineering, Tiruchengode, India.*

ARTICLE INFO

Article history:
Received 20 October 2013
Received in revised form 21 November 2013
Accepted 22 November 2013
Available online 15 December 2013

Keywords:
Glaucoma, texture, quantization level, back propagation.

ABSTRACT

Glaucoma is a multifactorial optic neuropathy characterized by elevated intraocular pressure. As the visual loss caused by the disease is irreversible, early detection is essential. Fundus images are taken as input and it is preprocessed using histogram equalization. First order features from histogram and twenty-two second order features from Gray Level Co-occurrence Matrix (GLCM) are extracted from the preprocessed image as textural features reflects physiological changes in the fundus images. Second order textural features are extracted for different quantization levels viz 8 and 16 in 0° orientation for unit distance. Extracted features are selected using Sequential Forward Floating Selection (SFFS) and fed as input to back propagation network to classify the images as normal and abnormal.The proposed computer aided diagnostic system achieved 92% sensitivity, 94% specificity, 93% accuracy and can be used for screening purposes.

To Cite This Article: S. Karthikeyan, Dr. N. Rengarajan, Analysis of Gray Levels for Retinal Image Classification. ***Aust. J. Basic & Appl. Sci.,*** *7(13): 58-65, 2013*

INTRODUCTION

Glaucoma is the second leading cause of blindness. A survey shows that the glaucoma is responsible for 6 million cases worldwide. The main risk factor of glaucoma is elevated pressure in the eye which causes damage to the eye optic nerve. It also affects the optic disc by enlarging the cup size. Early diagnosis and appropriate treatment can prevent permanent vision loss.

Many studies have been conducted for the early diagnosis of glaucoma. A novel Glaucoma Risk Index (GRI) was described by Rudiger Bock *et al*. (2010). The accuracy of 80% has been achieved in a 5-fold cross-validation setup and the GRI gains an area under ROC (AUC) of 88%. Fink *et al*. (2008) proposed an Independent component based image analysis and k-nearest neighbor classifier system for glaucoma classification and achieved a classification rate of 91%.

Texture is an innate property of virtually all surfaces. It contains important information about the structural arrangement of surfaces and their relationship to the surrounding environment. The textural properties of images appear to carry useful information for discrimination purposes and hence texture analysis of fundus image is performed. Haralick *et al*. (1973) used a class of quickly computable textural features in category identification tasks of three different kinds of image data. Accuracy on independent test sets are 89% for the photomicrograph image set, 82% for the aerial photographs and 83% for the satellite imagery.

Andree Baraldi and Flavio Parmiggiani (1995) investigated the statistical meaning of the six GLCM parameters. Two parameters, energy and contrast are considered to be the most efficient for discriminating different textural patterns. A novel glaucoma detection system using a combination of texture and higher order spectra features proposed by Rajendra Acharya *et al* (2011) provided an accuracy of more than 91%.

Yogesh Kumar and Sasikala (2012) described texture analysis of retinal layers in spectral domain OCT in which diagnosis of age related macular degeneration, diabetic macular edema and central serous retinopathy was tested. The behavior of co-occurrence statistics was investigated by W. Gomez *et al* (2012) to classify breast ultrasound (BUS) images. The best AUC of 0.81 was achieved with 32 gray levels and 109 features and AUC of 0.87 was obtained regarding the single texture features. The texture descriptors that contributed notably were contrast and correlation.

This paper presents the behavior of texture features, as a function of gray-level quantizations to classify retinal fundus images. The paper is structured as follows: Section II describes the dataset and proposed method. Section III describes experimental results which indicate that the proposed features should be useful for

Corresponding Author: S. Karthikeyan, Associate Professor, Department of ECE, K.S.R. College of Engineering, Tiruchengode, India.
E-mail: skkn03@gmail.com

glaucoma diagnosis. Discussion about analysis of gray levels were explained in chapter IV and Section V concludes the paper.

MATERIAL AND METHODS

Fig 1 describes the flow chart of the proposed method. A novel automated glaucoma detection system using texture features is used in this work. After preprocessing the acquired fundus images, texture based features are extracted and subjected to feature selection process. Subsequently, these features are fed to back propagation network for classification. Further an analysis on the influence of different features in the accuracy of glaucoma assessment is performed.

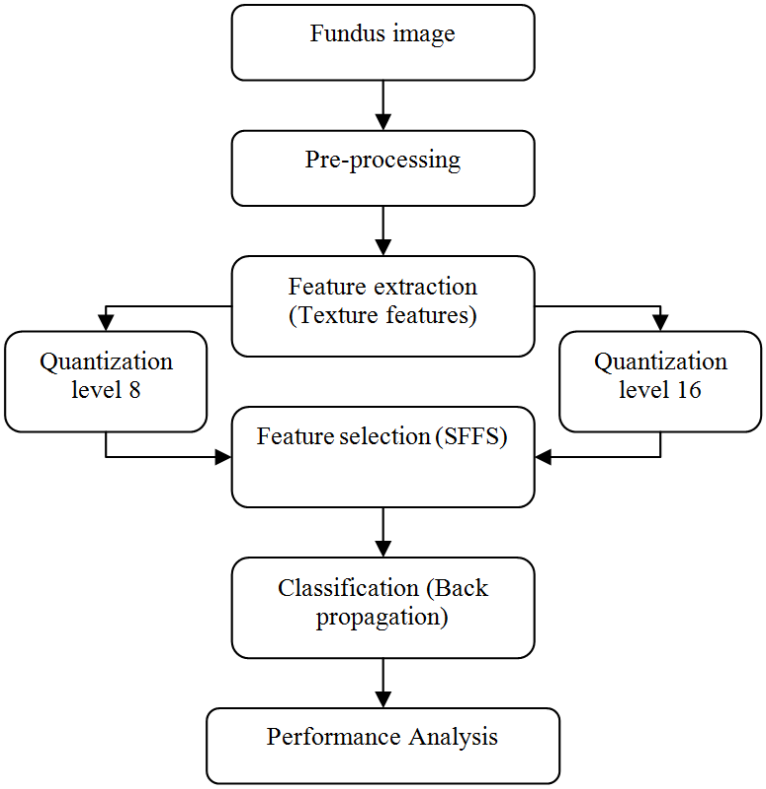

Fig. 1: Flowchart of the proposed method.

A. Data:

Fundus images used in this work are captured by Topcon TRC50 EX mydriatic fundus camera with a 50° field of view at Aravind Eye hospital, Madurai. The image size is 1900x1600 pixels at 24 bits true color image. Doctors in the ophthalmic department of the hospital approved the images for the research purpose. Various stages of glaucoma fundus images are also taken from optic-disc.org, a public database.

B. Preprocessing:

The retinal images are pre-processed for improving the local contrast of an image and bringing out more detail. Muthu Rama Krishnan and Oliver Faust (2013) described that the contrast is improved by increasing the dynamic range of the image histogram. Histogram equalization enhances the contrast of images by transforming the values in an intensity image and the equalized image is shown in Fig.2.

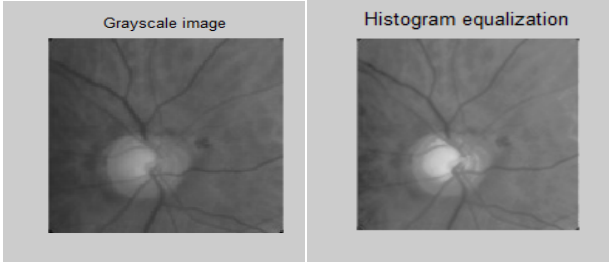

Fig. 2: Grayscale fundus image and histogram equalized image.

Australian Journal of Basic and Applied Sciences, 7(13) November 2013, Pages: 58-65

C. Texture Features:

Texture is a result of local variations in brightness within one small region of an image. Aminah Naseri *et al*. (2012) suggested that if the intensity values of an image are thought of as elevations, then texture is a measure of surface roughness. To measure the physiological changes in the fundus image due to the glaucomatous damage, texture analysis is performed. When the optic nerve is damaged by glaucoma, many of the individual nerve fibres that make up the nerve are lost and the optic nerve becomes excavated and grows larger leading to the differences in respective fundus images. Statistical methods are used here to analyze the spatial distribution of gray values by computing local features at each point in the image and to derive a set of statistics from the distributions of the local features.Depending on the number of pixels defining the local feature, statistical methods can be further classified into first order (one pixel), second-order (two pixels) and higher-order (three or more pixels) statistics. Two sets of statistical textural features namely first-order statistics computed using histogram based approach and second-order statistics computed from spatial gray-level occurrence matrix are used to characterize the type of retinal image. First order features namely mean, standard deviation, skewness, kurtosis and entropy are extracted from the preprocessed image. The gray-level co-occurrence matrix (GLCM) proposed by Haralick *et al*. (1973) is calculated to provide a second order method for generating texture features. Twenty two texture features namely autocorrelation, contrast, correlation I, correlation II, cluster prominence, cluster shade, dissimilarity, energy, entropy, homogeneity I, homogeneity II, maximum probability, sum of squares, sum average, sum entropy, sum variance, difference variance, difference entropy, information measure of correlation I, information measure of correlation II, inverse difference normalized and inverse difference moment normalized are extracted from the GLCM matrix. The process is continued regarding two quantization levels (8 and 16) for orientations of 0°. Thus two co-occurrence matrices were obtained and 22 textural features are extracted from each matrix.

D. Feature Selection:

High dimension data could contain high degree of redundant information, which may degrade the efficiency of the system. Hence feature selection process is performed using Sequential Floating Forward selection (SFFS) feature selection method. This method is used to deal with the nesting problem. The best subset of features is initialized as the empty set and at each step a new feature is added as described by Jain A. K and Zongker (1997). Then the algorithm searches for features that can be removed until the correct classification error does not increase. This algorithm is a combination of the sequential forward and the sequential backward methods. The "best subset" of features is constructed based on the frequency with which each attribute is selected in the number of repetitions given. The selected features are used for the classification process.

E. Classification:

Back propagation is used for the classification of the selected features. J.A. Anderson (1995) described that back propagation is a common method of training artificial neural networks. From a desired output, the network learns from many inputs. It is a supervised learning method and is a generalization of the delta rule. It requires a dataset of the desired output for many inputs, making up the training set. It is most useful for feed-forward networks. Back propagation requires that the activation function used by the artificial neurons be differentiable. In BP algorithm iterative updating of weights based on the error signal carries out training. Negative gradient of a mean squared error function is used. In the output layer, the error signal is multiplied by the slope of the activation function. Extracted statistical parameters are normalized and are used in the training of BP network and the resultant trained network is used for testing.

III. Results:

The experiment results obtained for first and second order textural features were presented in the form of tables and Fig as follows: Extracted first order feature statistics for sixteen images comprising normal, early and advanced stages are shown in Table 1.

In the Table 1, first six images used are normal images and the remaining ten images refers to the abnormal images with early and advanced stages. Fig 3 describes the statistical values for various first order features.

Since mean and standard deviation are purely intensity based features, they are sidelined by the optimization algorithm. Energy is also directly dependent on the statistical property of the input data and hence it is least preferred over skewness, kurtosis and entropy. Entropy and kurtosis does not give a clear differentiation of the normal and abnormal classes and show overlapping of values. Discrimination between normal and abnormal images using kurtosis feature is not appreciable. Skewness, the third central moment μ_3 is the measure of the asymmetry of the data around the sample mean.If skewness is negative, the data are spread out more to the left of the mean than to the right. There is a clear discrimination between normal and abnormal classes using skewness. Few features namely contrast, homogeneity, energy, correlation and entropy are compared for a few images and are shown in Fig 4.

Australian Journal of Basic and Applied Sciences, 7(13) November 2013, Pages: 58-65

Table I: First order statistical features for few images.

Image. No	Image Type	Mean	Standard Deviation	Skewness	Kurtosis	Entropy
1	Normal	0.72	0.294	-0.623	0.447	0.614
2		0.76	0.276	-0.685	0.468	0.527
3		0.81	0.254	-0.690	0.498	0.436
4		0.82	0.243	-0.732	0.399	0.594
5		0.83	0.212	-0.794	0.431	0.582
6		0.89	0.190	-0.810	0.388	0.590
7	Early	0.95	0.412	0.212	0.446	0.82
8		0.87	0.493	0.284	0.365	0.816
9		0.78	0.521	0.326	0.487	0.79
10		0.89	0.518	0.494	0.436	0.92
11		0.76	0.573	0.584	0.498	0.95
12	Advanced	0.87	0.32	0.576	0.381	0.52
13		0.92	0.39	0.50	0.428	0.59
14		0.82	0.41	0.543	0.391	0.63
15		0.86	0.44	0.596	0.459	0.69
16		0.91	0.49	0.612	0.440	0.72

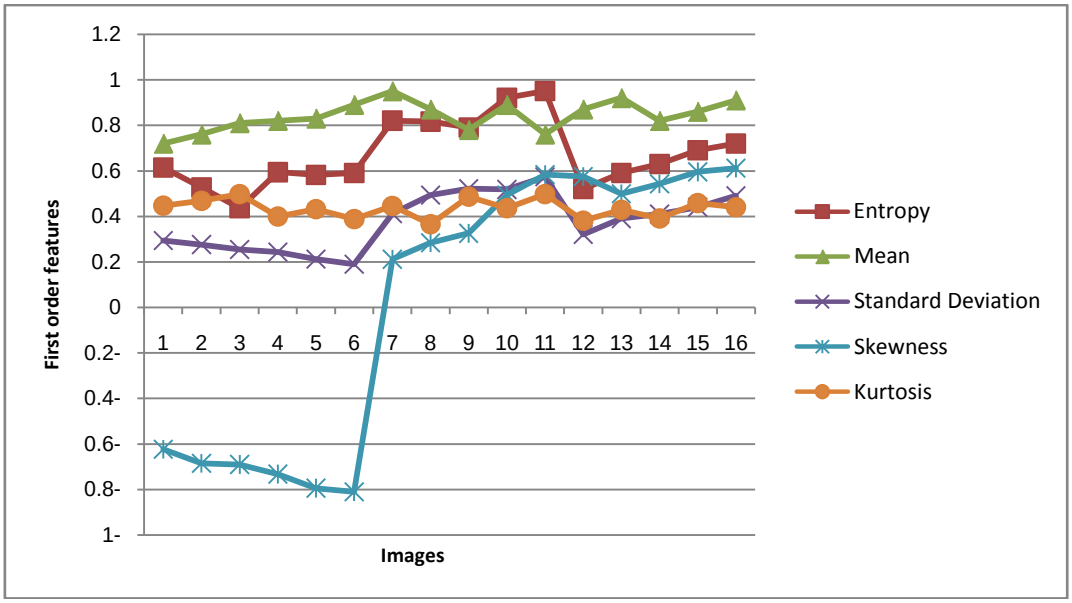

Fig. 3: First order features for sample images.

Fig. 4: Second order features for sample images.

Contrast feature represents the local variations present in the image. In case of retinal images due to the enlargement in the cup region the intensity values of the cup are highly distinguishable and contrast feature has higher values in abnormal images. High contrast values imply high contrast texture. The value of the entropy is low if the same pair of pixels appears frequently and high if all the grayscale are faintly represented. Energy is preferred to entropy since the elements in this category measure texture different from contrast.

Homogeneity value is dependent on the gray scale value of the pixels that have similar intensities. In region of interest enclosing the cup region, intensity value is more contributing to the increased value of homogeneity. hen a large number of pixels of similar intensity exist together, homogeneity is higher. High correlation values close to 1 imply a linear relationship between the gray levels of pixel pairs. Correlation reaches its maximum regardless of pixel pair occurrence as high correlation can be measured either in low or high energy. Correlation feature is almost identical in normal and abnormal cases. Entropy features show overlapping of values. Out of the features presented, the best features were observed to be contrast, energy and homogeneity.

Table II: Result of gray level 8.

Features	Normal image	Abnormal image
Autocorrelation	70.2527±2.5996	62.8439±19.65
Contrast	0.5232±0.1347	1.0604±0.2063
Correlation I	0.9076±0.0116	0.8821±0.0169
Correlation II	0.9076±0.0116	0.8821±0.0169
Cluster prominence	500.51±134.80	997.67±579.14
Cluster shade	15.8089±4.8111	-11.8421±27.88
Dissimilarity	0.3945±0.0686	0.5523±0.0729
Energy	0.0927±0.0204	0.1563±0.1987
Entropy	2.8897±0.1983	3.3279±0.2720
Homogeneity I	0.8209±0.0264	0.7733±0.252
Homogeneity II	0.8151±0.0282	0.7635±0.0276
Maximum probability	0.1835±0.0457	0.1183±0.0320
Sum of squares	70.4552±2.6776	93.2052±19.78
Sum average	16.4438±0.3431	18.7151±2.0984
Sum entropy	206.07±9.6904	276.03±62.3855
Sum variance	2.4824±0.1255	2.7620±0.1913
Difference variance	0.5233±0.1348	1.0604±0.2063
Difference entropy	0.7887±0.0713	0.9519±0.0723
Information measure of correlation I	-0.4775±0.0317	-0.4446±0.0177
Information measure of correlation II	0.9141±0.0103	0.9215±0.0128
Inverse difference normalized	0.9772±0.0039	0.9689±0.0040
Inverse difference moment normalized	0.9979±0.005	0.9961±0.0007

Table III: Result of gray level 16.

Features	Normal image	Abnormal image
Autocorrelation	19.6724±0.6426	25.1933±4.7872
Contrast	0.1966±0.0369	0.3208±0.0532
Correlation I	0.8587±0.0170	0.8451±0.0239
Correlation II	0.8587±0.0170	0.8451±0.0239
Cluster prominence	27.6587±7.3438	50.5154±29.2446
Cluster shade	1.7675±0.4431	-1.3265±2.8259
Dissimilarity	0.1887±0.0300	0.2552±0.0343
Energy	0.2492±0.0332	0.1824±0.0444
Entropy	1.7924±0.1443	2.1351±0.2289
Homogeneity I	0.9069±0.0139	0.8810±0.0152
Homogeneity II	0.9064±0.0143	0.8786±0.0156
Maximum probability	0.3764±0.0375	0.3053±0.0704
Sum of squares	19.6341±0.6641	25.1782±4.8057
Sum average	8.7327±0.1546	9.8039±0.9765
Sum entropy	52.9257±2.6862	67.2203±12.9962
Sum variance	1.6420±0.1134	1.8955±0.1674
Difference variance	0.1966±0.0370	0.3208±0.0531
Difference entropy	0.4945±0.0492	0.6115±0.0475
Information measure of correlation I	0.5212±0.0332	-0.4912±0.0202
Information measure of correlation II	0.8462±0.0181	0.8651±0.0263
Inverse difference normalized	0.9791±0.0032	0.9723±0.0036
Inverse difference moment normalized	0.9970±0.0005	0.9952±0.0008

Table IV: Performance measure of gray levels.

Gray levels	Sensitivity	Specificity	Accuracy
8	90%	92%	91%
16	92%	94%	93%

Australian Journal of Basic and Applied Sciences, 7(13) November 2013, Pages: 58-65

The test performance of the back propagation model determined by the computation of the statistical parameters such as sensitivity, specificity and classification accuracy are defined as follows. Fig. 5 describes the performance analysis of gray levels. Sensitivity is a measure that determines the probability of results that are true positive such that a person has disease. It is the ratio of number of correctly classified glaucoma subjects to the total number of glaucoma patients.

$$\text{Sensitivity} = \frac{TP}{(TP+FN)} \tag{1}$$

True Positives (TP) denotes the number of glaucoma images correctly detected and False Negatives (FN) refers to the number of glaucoma images that were detected as normal images. Specificity is a measure that determines the true negatives that a person is not affected by the disease. It is the ratio of number of correctly classified normal subjects to the total number of normal subjects. True Negatives (TN) denotes the number of normal images correctly identified and False Positives (FP) refers to the number of normal images that were detected as glaucoma images.

$$\text{Specificity} = \frac{TN}{(TN+FP)} \tag{2}$$

Classification accuracy is the ratio of the total number of correctly classified images to the total number of images taken for classification.

$$\text{Accuracy} = \frac{(TP+TN)}{(TP+FP+TN+FN)} \tag{3}$$

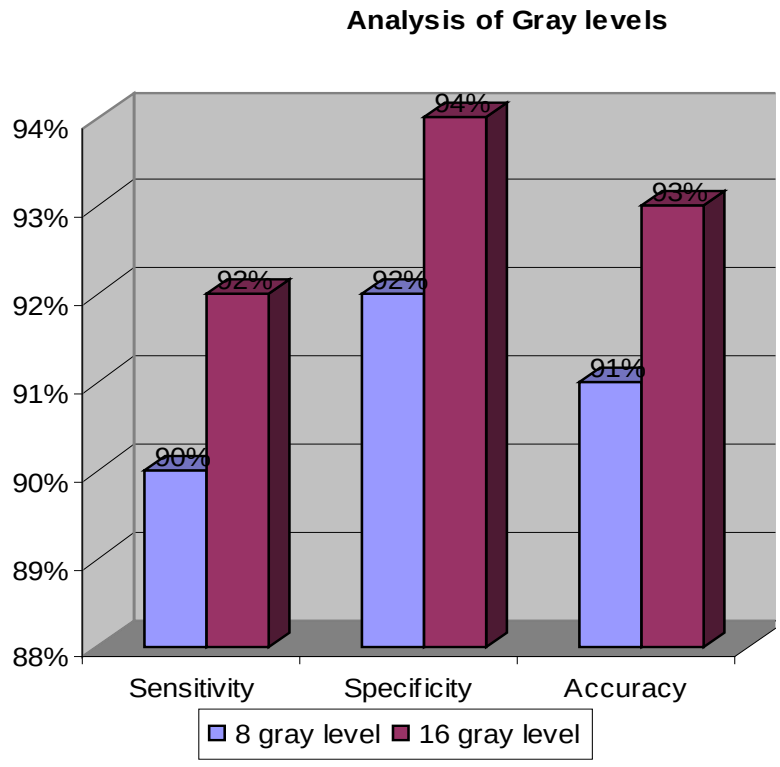

Fig. 5: Classification result analysis of 8 and 16 gray levels.

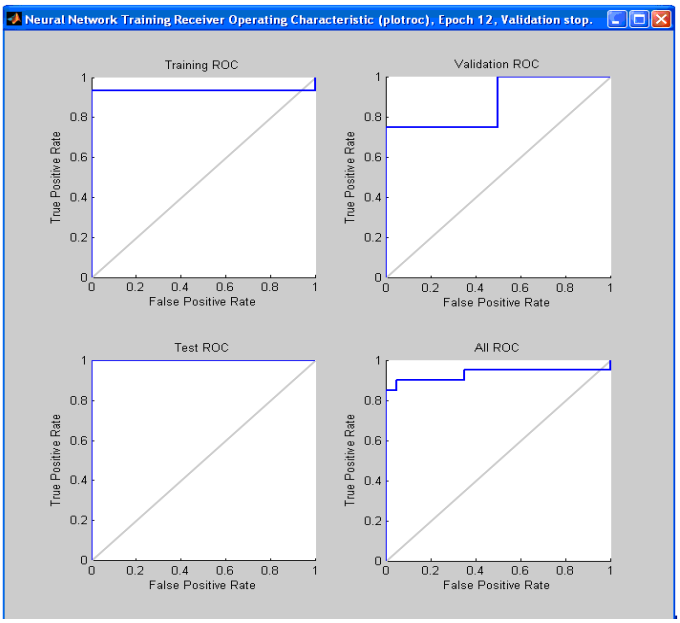

Fig. 6: Neural network output.

IV. Discussion:

The correct classification rates of the stand alone neural network were 92% for normal subjects and 94% for glaucoma patients. The total classification accuracy in neural network was 93% and the area under convergence plot is shown in Fig 6. Except skewness feature, the first order features showed poor discrimination between the images since first order features only characterize the brightness and not its spatial structure. Skewness has a negative value for normal images and positive value for early and advanced stage of the disease. This feature does not involve any overlapping of the class and serves as a good feature to improve interclass discrimination. Only skewness value showed promising results in classifying the images and there was no overlapping of classes. Second order features exhibits discriminatory character for each of the images and when tested with the classifier provides 94% sensitivity and 92% specificity. Contrast feature showed higher variation for glaucoma images as compared to normal fundus images.

V.Conclusion:

This work presents a study of co-occurrence texture statistics as a function of gray-level quantization for glaucoma diagnosis. The retinal images were preprocessed for improving the local contrast of an image and bringing out more detail. Twenty-two texture features autocorrelation, contrast, correlation I, correlation II, cluster prominence, cluster shade, dissimilarity, energy, entropy, homogeneity I, homogeneity II, maximum probability, sum of squares, sum average, sum entropy, sum variance, difference variance, difference entropy, information measure of correlation I, information measure of correlation II, inverse difference normalized and inverse difference moment normalized extracted from the GLCMs were extracted regarding two quantization levels 8 and 16 for 0° orientations for unit distance. Sequential Forward Floating Selection (SFFS) was used for feature selection. The selected features were fed as input to back propagation network to classify the images as normal and abnormal. Features computed from GLCM with orientation of 0° and of quantization level 16 contributed notably to discriminate between normal and abnormal fundus images. The proposed computer aided diagnostic system achieved 92% sensitivity, 94% specificity, 93% accuracy and can be used for screening purposes.

REFERENCES

Bock, R., J. Meier, L.G. Nyúl, J. Hornegger, G. Michelson, 2010. Glaucoma risk index: Automated glaucoma detection from color fundus images. Medical Image Analysis, 14(3): 471-481.

Fink, F., K. Worle, P. Gruber, A.M. Tome, J.M. Gorriz-Saez, C.G. Puntonet, E.W. Lang, 2008. ICA Analysis of Retina Images for Glaucoma Classification. In the Proceedings of the 30th Annual International Conference of IEEE EMBS, pp: 4664-4667.

Robert, M., Haralick, K. Shanmugam and Itshak Dinstein, 1973. Textural Features for Image Classification. IEEE Transactions on Systems, Man and Cybernetics, 3(6): 610-621.

Andrea Baraldi and Flavio Panniggiani, 1995. An Investigation of the Textural characteristics associated with Gray Level Co-occurrence Matrix Statistical Parameters. IEEE Transactions on Geoscience and Remote Sensing, 33(2): 293-304.

Rajendra Acharya, U., Sumeet Dua, Xian Du, S. Vinitha Sree and Chua Kuang Chua, 2011. Automated Diagnosis of Glaucoma Using Texture and Higher Order Spectra Features.IEEE Transactions on Information Technology In Biomedicine, 15(3): 449-455.

Yogesh Kumar, A., M. Sasikala, 2012. Texture Analysis of Retinal Layers in Spectral Domain OCT Images. International Journal of Emerging Technology and Advanced Engineering, 2(12): 296-300.

Gomez, W., W.C.A. Pereira and A.F.C. Infantosi, 2012. Analysis of Co-Occurrence Texture Statistics as a Function of Gray-Level Quantization for Classifying Breast Ultrasound. IEEE Transactions on Medical Imaging, 31(10): 1889-1899.

Muthu Rama Krishnan, M., Oliver Faust, 2013. Automated glaucoma detection using hybrid feature extraction in retinal fundus images. Journal of Mechanics in Medicine and Biology, 13(1): 1350011-21.

Amineh Naseri, Ali. Pouyan, Nader. Kavian, 2012. Automated detection of retinal layers using Texture Analysis. International Journal of Computer Applications, 46(1): 29-33.

Jain, A.K. and Zongker, 1997. Feature selection: Evaluation, application, and small sample performance.IEEE Trans. Pattern Anal. Mach. Intell., 19(2): 153-158.

Anderson, J.A., 1995. An Introduction to Neural Networks. Cambridge, MA: MIT Press.